ANALYTICAL BIOCHEMISTRY 224, 83–91 (1995)

A Fluorescence Quench and Dequench Assay of Fibrinogen Polymerization, Fibrinogenolysis, or Fibrinolysis

Jung-He Wu and Scott L. Diamond[1]

Bioengineering Laboratory, Department of Chemical Engineering, 907 Clifford C. Furnas Hall, The State University of New York, Buffalo, New York 14260

Received July 8, 1994

We present a kinetic assay based on the use of fluorescein isothiocyanate (FITC)-labeled fibrinogen as a fluoroactive substrate. The multiple FITCs bound to fibrinogen experienced quenching due to their close proximity. The thrombin-induced polymerization of FITC-fibrinogen led to additional fluorescence quenching due to enhanced neighbor–neighbor interactions in protofibrils and protofibril aggregates. The initial rate of quenching was directly dependent on the thrombin concentration at either low or high ionic strength. The final extent of quenching during polymerization with thrombin could be modulated by prevailing ionic strength and thrombin concentration suggesting that the quenching was due to fibril extension as well as aggregation. The full extent of quenching was greatly reduced by addition to the reaction of unlabeled fibrinogen or Gly-Pro-Arg-Pro, as expected for quenching due to neighbor–neighbor interactions. In contrast to polymerization, cleavage of fibrinogen by plasmin released FITC-labeled fragments free of proximity-based quenching that resulted in a large intensity increase as lysis proceeded—a process termed dequenching. The majority of the dequenching signal during fibrinogenolysis occurred during the generation of fragment X which proceeded as a first-order process with respect to fibrinogen-bound plasmin with $k_{cat} = 0.479\ s^{-1}$. The K_d of active plasmin to fibrinogen was calculated to be 0.42 μM. Addition of ε-aminocaproic acid (εACA)–plasmin complex to FITC–fibrinogen produced little dequenching, demonstrating a requirement for binding in order to initiate lysis. Also, addition of excess εACA after plasmin-mediated fibrinogenolysis was initiated resulted in a dose-dependent inhibition of dequenching, indicating that plasmin can be desorbed from fibrinogen either by εACA disruption of the fibrinogen–plasmin complex or by εACA capture of desorbing plasmin. Similar to fibrinogenolysis, dequenching occurred in a plasmin-dependent manner during lysis of polymerized fibrin fibers in suspension. The use of fluorescently labeled fibrinogen as a fluoroactive substrate for plasmin or thrombin will allow kinetic analysis of very dilute systems where (i) the presence of the lysine binding sites and (ii) steric phenomena are critical—two situations where small chromogenic peptide substrates are unsuited.

Chromogenic and fluorogenic substrates have been widely used to assay the activity of proteases such as plasmin (1). These substrates are small peptides with a relatively low-affinity interaction with plasmin (K_m > 100 μM) and are cleaved rapidly by plasmin ($k_{cat} \sim 10$–$40\ s^{-1}$). Although useful, chromogenic substrates do not directly yield kinetic information regarding the action of fibrin-bound plasmin on cleavage sites within the α, β, and γ strands of fibrin(ogen). Given the competition of glu- and lys-plasminogen and glu- and lys-plasmin for lysine binding sites (LBS)[2] in fibrin and LBS generation during lysis (2–4), kinetic analysis of these complex reaction mixtures would benefit from substrates that allow binding while simultaneously producing a signal related to cleavage events.

The complex and dynamic nature of fibrin(ogen)olysis has prevented quantitative kinetic analysis, although the reaction pathway is well established (5–7). Briefly, plasmin binds fibrinogen (340 kDa) and initially cleaves several sites in the C-terminus of the α chains of fibrinogen and the $\beta(Arg_{42}–Ala_{43})$ bonds to yield fragment X (240–265 kDa). The cleavage of a $\gamma(Lys_{62}–Arg_{63})$ bond in late fragment X—which has cleaved $\alpha(Lys_{81}–Asp_{82})$ or $\alpha(Arg_{103}–Asp_{104})$ and $\beta(Lys_{122}–Asp_{123})$ or $\beta(Lys_{133}–$

[1] To whom correspondence should be addressed. Fax: (716) 645-3822.

[2] Abbreviations used: LBS, lysine binding sites; FITC, fluorescein isothiocyanate; BSA, bovine serum albumin.

0003-2697/95 $6.00

Asp_{134}) bonds—yields fragment Y (155 kDa) and fragment D (70–100 kDa). Finally, the cleavage of the second $\gamma(Lys_{62}–Arg_{63})$ bond of fragment Y results in the generation of fragment E (50 kDa) and the second fragment D, both of which can undergo further degradation. During fibrin(ogen) degradation, plasmin can cleave over 30 cleavage sites in a fairly specific order (8) while generating additional lysine binding sites. About 10 of these cleavage sites are considered kinetically significant (9). It has been observed that under some conditions coarse fibers of fibrin lyse faster than fine fibers (10). These multiple processes contribute to the complexity of kinetic analysis and the reliance on lumped indicators such as percentage lysis to indicate solubilization. An added complexity to the kinetic study of lytic processes is the presence of cryptic binding sites in fibrinogen that are revealed in intact fibrin as well as the different affinity of plasminogen toward fibrin and fibrinogen. The kinetics and mechanisms of fibrinogenolysis and fibrinolysis are different. During later stages of lysis, as the contributions of carboxy terminal lysine binding sites become important, the kinetics of fibrinogenolysis and fibrinolysis may share some common aspects.

The basic mechanisms and kinetics of fibrin polymerization and fibrin structure formation are well studied (11,12). In general, thrombin releases fibrinopeptide A with subsequent protofibril extension of staggered monomers with an equivalent of two monomers per unit length of protofibril. The slower release of fibrinopeptide B by thrombin is associated with lateral aggregation to form thick fiber bundles containing many protofibrils. Under high salt conditions (0.3 M NaCl) the rate of protofibril extension is kinetically favored leading to a transparent (fine) gel of thin fibers (13–15). Physiological levels of salt (0.1 M NaCl) allow for aggregation events to compete successfully with protofibril extension, resulting in turbid (coarse) gels. Polymerization at low levels of thrombin or elevated Ca^{2+} levels results in thicker fibers (13,16). Within the fiber, the density of fibrin is about 210 mg/ml for fine fibers (17) and 280 mg/ml for coarse fibers (14,17). This fibrin density is almost two orders of magnitude greater than the bulk concentration of fibrinogen which is 3 mg/ml (8.8 μM) in plasma prior to polymerization.

An additional challenge in studying fibrinolytic rates is the heterogeneous nature of a fibrin gel. Significant time is required for proteins to diffuse into gels or clots and kinetic measurements under these conditions likely contain diffusion limitations (18,19). Pressure-induced permeation of lytic agents into fibrin helps to overcome these limitations and leads to large enhancement of fibrinolysis (20). Kinetic studies of fibrinolysis are most easily analyzed in well-mixed systems that do not contain concentration gradients. Dilute suspensions of fibrin fibers are suited for this purpose and have been used (21,22) for kinetic analysis. Fiber suspensions provide a suitable approach for the study of intrinsic kinetics without influence of the rates of diffusion and permeation through fibrin structures.

We present a kinetic assay based on the use of fluorescein isothiocyanate (FITC)-labeled fibrinogen as a fluoroactive substrate. The multiple FITCs bound to fibrinogen experienced quenching due to their close proximity as first noted by Genton *et al.* (23). Cleavage of fibrinogen by plasmin releases FITC-containing peptide fragments that were free of proximity-based quenching, resulting in a large intensity increase as lysis proceeded—a process termed dequenching. In contrast, thrombin-induced polymerization of FITC–fibrinogen led to fluorescence quenching due to enhanced neighbor–neighbor interactions in protofibrils and protofibril aggregates. The extent of quenching during polymerization with thrombin was dependent on the extent of protofibril extension and aggregation. By exploiting fluorescence quenching, fluorescently labeled fibrinogen can be used as a fluoroactive substrate for plasmin or thrombin. In this approach, binding and macromolecular structures of fibrin and fibrinogen are maintained and kinetic phenomena can be studied in well-mixed systems at nanomolar concentrations.

MATERIALS AND METHODS

Reagents

Purified human thrombin (Sigma) was obtained as a lyophilized powder (specific activity: 3000 NIH U/mg). The thrombin was dissolved in high-purity water at 200 NIH U/ml, aliquoted, and frozen at −75°C. Lyophilized human fibrinogen (grade L, Kabi AB) was dissolved in 0.05 M tris(hydroxymethyl)aminomethane (Tris–HCl), pH 7.4, and dialyzed at 4°C against 0.05 M Tris–HCl containing 0.1 or 0.3 M NaCl for 18 h with 1-liter changes every 6 h. The solution was centrifuged at 2000*g* for 20 min (4°C) and the supernatant was frozen in small aliquots at −75°C. Purified human plasmin (American Diagnostica Inc.) was reconstituted, centrifuged at 2000*g* for 20 min (4°C), and stored at −75°C. Fluorescein isothiocyanate, isomer I (FITC) was obtained from Molecular Probes. For the labeling reaction (24), fibrinogen (10 mg/ml) was incubated with FITC (1 mg/ml) with continuous stirring for 1 h at 22°C in a labeling buffer of 0.1 M sodium bicarbonate (pH 9.0). The reaction was stopped with hydroxylamine (0.15 M final concentration) after which the FITC–fibrinogen was dialyzed extensively in the dark at 4°C and stored at −75°C. Nonreduced FITC–fibrinogen had an apparent size of 320 to 340 kDa as indicated by SDS/PAGE. Reduction of FITC–fibrinogen produced full-length α, β, and γ chains of 67, 55, and 47 kDa, respectively, indicating the molecular integrity of the α chain in the preparation.

SDS/PAGE and Fluorescence Scanning

Small samples were removed from fibrinogenolytic reactions at various times and promptly heated at 95°C for

5 min in SDS running buffer [TE buffer (pH 8.0), 2% (v/v) SDS, 8 M urea, ± 1% (v/v) β-mercaptoethanol]. The samples were run on 0.5-mm-thick, 4 to 15% polyacrylamide gels (Pharmacia PhastGel) and scanned using an epifluorescence microscope with a 10× objective (Leitz Aristoplan). The fluorescence emission was directed at an intensified CCD camera (Dage MTI), recorded digitally using an 8-bit frame grabber (Data Translation, Inc.), and evaluated using NIH Image 1.49 software. Following fluorescence scanning, the gels were developed using a silver staining kit (Pierce, Inc.) according to manufacturer's instructions and analyzed using scanning densitometry.

Reaction Conditions and Fluorimetry

The buffer for polymerization and lysis experiments contained 0.1 or 0.3 M NaCl, 0.05 M Tris–HCl, 5 mM $CaCl_2$. Cuvettes were preincubated with 10 μM BSA for 30 min to minimize adsorption. FITC–fibrinogen had stable fluorescence emission with little variation for several hours. To produce suspensions of fibrin fibers, thrombin (final concentration 1 U/ml) was mixed (for 5 s) into dilute fibrinogen (80 nM) solutions at 0.1 or 0.3 M NaCl after which the polymerization was monitored until fluorescence quenching was complete and stable for 1 h. The daily-made fiber suspensions yielded a highly repeatable extent of quenching and were stable for several hours as indicated by the stability of the fluorescence signal. Small volumes of the fiber suspension were then pipetted into 2.4 ml of the reaction buffer and monitored for 200 to 400 s to establish the fluorescence baseline before addition of plasmin or other reagents. Fluorescence was measured in a Perkin–Elmer LS-50 luminescence spectrometer.

We have carried out structural evaluation of these fibrin suspensions. Using epifluorescence microscopy or digitally enhanced DIC microscopy (100×, 1.32 NA planapo objective lens with 1.4 NA oil immersion condenser), we visualized the fibrin formed during polymerization of dilute fibrinogen solutions. Long, thin fibrin fibers with lengths of 5 to 20 μm were easily visualized by epiflourescence. The diameter of these fibers was likely less than ~100 nm since they were just barely visible by contrast-enhanced DIC microscopy. We also observed loose aggregated forms (~10 μm in size) of fibers, but these loose structures would not be expected to hinder enzyme penetration into the aggregate.

RESULTS

Fibrinolysis or fibrinogenolysis is a multistep and heterogeneous reaction process which includes the transport by diffusion or permeation of the enzyme into fibrin, the binding of reactive species to fibrin, and irreversible catalytic reactions on the solid fibrin phase. In this study, the reactions occurred under well-mixed conditions. Addition of 10 nM of plasmin to 20 nM of FITC–fibrinogen resulted in an immediate increase in fluorescence emission, reaching a final level that was 2.0-fold above the baseline intensity (Fig. 1). Addition of 1 U/ml of thrombin to 20 nM of FITC–fibrinogen caused an immediate quenching of the fluorescence emission to a final level that was 0.7 times the initial intensity. Addition of 10 nM plasmin to the polymerized fibrin caused immediate dequenching to a final extent that was identical to the final extent of dequenched degraded fibrinogen (Fig. 1). The FITC bound to fibrinogen experienced significant quenching as indicated by a red shift of 5 nm of maximum fluorescence emission compared to the maximum emission of pure FITC at 516 nm. We observed a repeatable blue shift (1.0 nm) during the breakup of fibrinogen under conditions of dequenching. This relatively small shift was likely due to the fact that the FITCs on the protein fragments remained fairly quenched compared to FITC in free solution. During polymerization of fibrinogen, red shifts were consistently observed but were less than 0.5 nm which also indicated that the FITC on the fibrinogen was quenched under resting conditions.

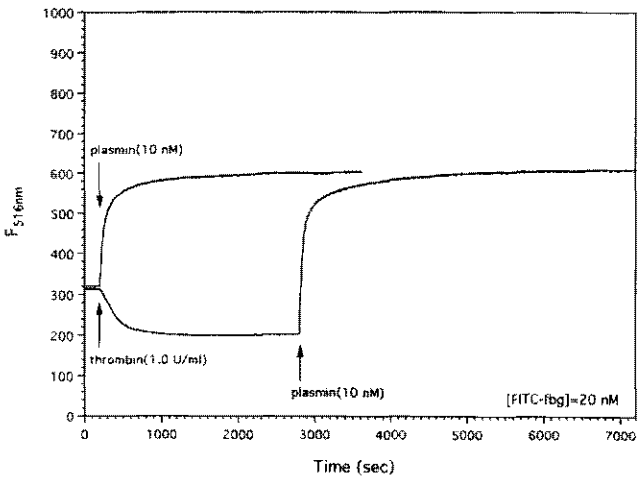

FIG. 1. Fluorescence intensity (at 516 nm) of 20 nM FITC–fibrinogen upon addition of 10.0 nM plasmin (top curve), demonstrating rapid dequenching that occurred during fibrinogenolysis. Rapid quenching was seen when 20 nM FITC–fibrinogen was polymerized by addition of 1.0 U/ml thrombin (bottom curve). The resulting quenched fibrin was rapidly degraded and dequenched upon addition of 10.0 nM plasmin, reaching a maximum fluorescence emission identical to that of degraded FITC–fibrinogen. Reaction conditions were 0.05 M Tris–HCl, 0.1 M NaCl, 5 mM $CaCl_2$ (pH 7.4, 22°C).

Fibrinogen Polymerization

The addition of thrombin to FITC–fibrinogen led to a rapid and dose-dependent reduction of fluorescence emission due to quenching. At these extremely low concentrations of species (<40 nM) the solutions were optically clear and the drop in fluorescence was not due to turbidity or scattering effects during polymerization.

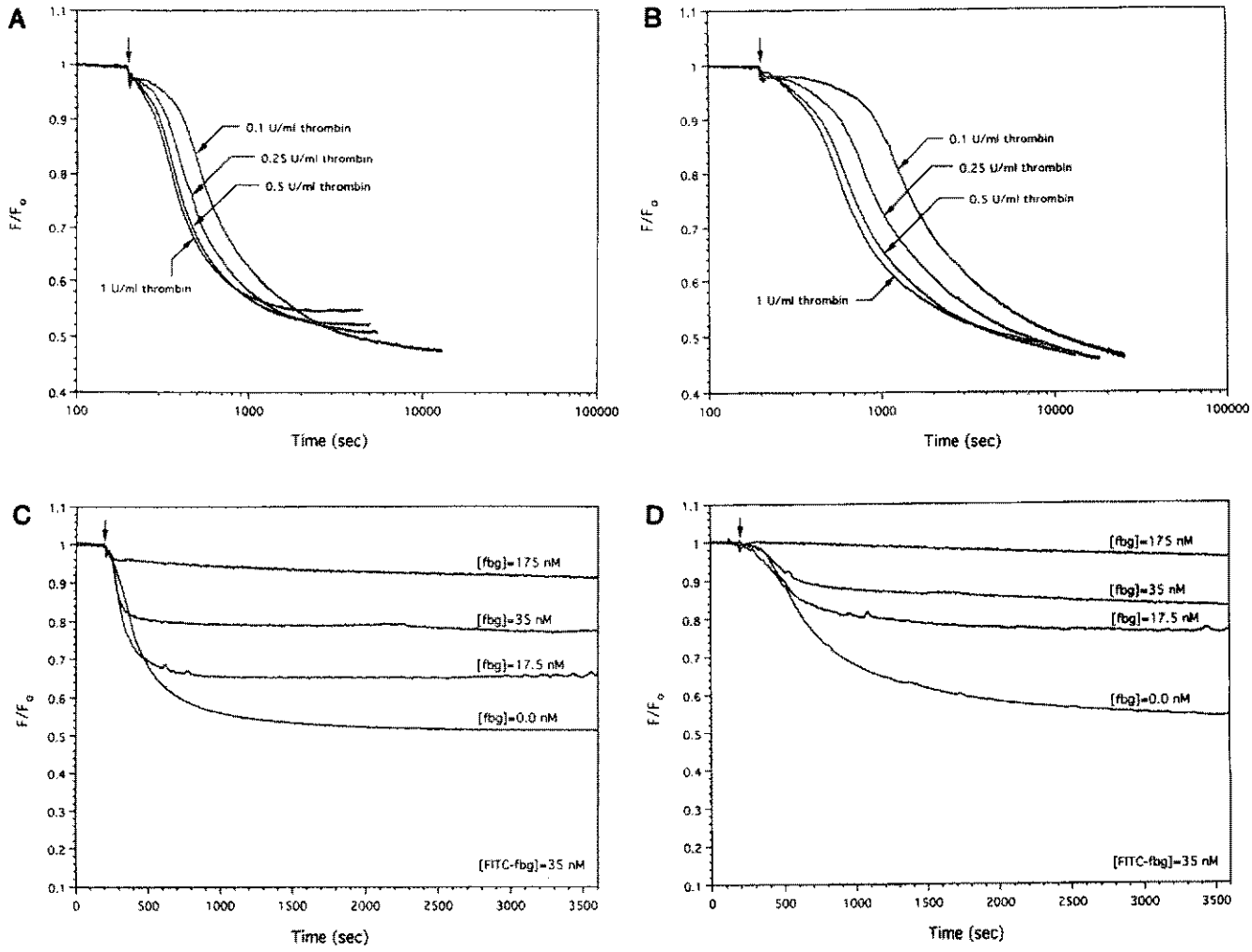

FIG. 2. Dependence of fluorescence intensity of 30 nM FITC–fibrinogen upon addition of 0.1 to 1.0 U/ml thrombin at 0.1 M NaCl (A) or 0.3 M NaCl (B). A slight and identical dilution of the reaction mixture occurred at 200 s with the addition of thrombin as indicated by the arrow. Fluorescence intensities were normalized by initial intensity to eliminate small variations (<3%) in the initial concentration of FITC–fibrinogen. Addition of varying amounts of unlabeled fibrinogen to 35 nM FITC–fibrinogen prior to addition of 0.5 U/ml thrombin resulted in a substantial attenuation in the final extent of quenching during polymerization of fibrinogen at 0.1 M NaCl (C) or 0.3 M NaCl (D).

Release of fibrinopeptide A and B by thrombin caused no dequenching of the FITC moieties on fibrin monomers. Also, the release of FPA and FPB by thrombin was not expected to cause quenching, which suggests that fibrinogen and fibrin monomers have the same fluorescence emission.

The initial rate of quenching was dependent on the initial concentration of thrombin for 30 nM fibrinogen polymerized at 0.1 M NaCl (Fig. 2A) or 0.3 M NaCl (Fig. 2B). At the lowest concentrations of thrombin used, a significant lag time was observed before dequenching proceeded. After the generation of sufficient monomer and protofibril extension, lateral aggregation of fibrils proceeded. Once dequenching began, the maximum rate of dequenching with time appeared to be largely independent of thrombin concentration as seen for similar maximum slopes on curves in Figs. 2A or 2B. Also, the final extent of quenching appeared to be modulated by the final thickness of the fiber. At low thrombin concentration and low salt, the thicker fibers that formed (after a significant lag) resulted in a greater final extent of quenching compared to the thinner fibers formed at high thrombin concentration (Fig. 2A). In high salt, which favors the formation of thin fibers, the modulation of the final extent of quenching by adjusting the thrombin concentration was qualitatively similar to the findings with low salt, but the final differences were much smaller. This may be due to the fact that fibers are relatively thin when formed at high salt conditions, their thickness only weakly dependent of thrombin concentration. However, at all thrombin concentrations, the lag phase was considerably longer in high salt buffer than that in

low salt, suggesting the importance of lateral aggregation during dequenching, since protofibril extension is fast at high salt conditions. This was consistent for polymerization conditions that favored protofibril extension and very thin fibers (>0.3 M NaCl, high thrombin, and low $CaCl_2$) which had very long lag phase, but ultimately produced a final extent of quenching similar to that seen in Figs. 2A and 2B (data not shown). When quenching achieved its maximal rate at a given stage of the polymerization, there was little difference between that rate for low and high salt concentrations.

The addition of unlabeled fibrinogen to the reacting mixture attenuated the thrombin-induced quenching in a dose-dependent manner (Figs. 2C and 2D)—the exact opposite would be expected for a scattering-based mechanism of loss of fluorescence signal. Increasing the concentration of unlabeled fibrinogen reduces the probability of two FITC–fibrin monomers either being incorporated sequentially in a protofibril or interacting within a given cross section of fiber. Increasing the unlabeled fibrinogen in the reaction altered the initial quenching rate slightly (at constant thrombin concentration) and reduced the final extent of quenching in a dose-dependent manner. At 5:1 ratio of unlabeled to labeled fibrinogen, the quenching during polymerization was completely eliminated in fine fibers (Fig. 2C) while a small amount of quenching occurred at this ratio during polymerization of coarse fibers (Fig. 2D). This is consistent with an increased probability of two or more labeled FITC–fibrin monomers quenching each other in a thick fiber cross section compared to the quenching probability in a thin fiber cross section which contains less fibrils. Thus, the quenching during polymerization is due to a mechanism involving molecular proximity which is achieved by two processes: fibril extension and fibril aggregation.

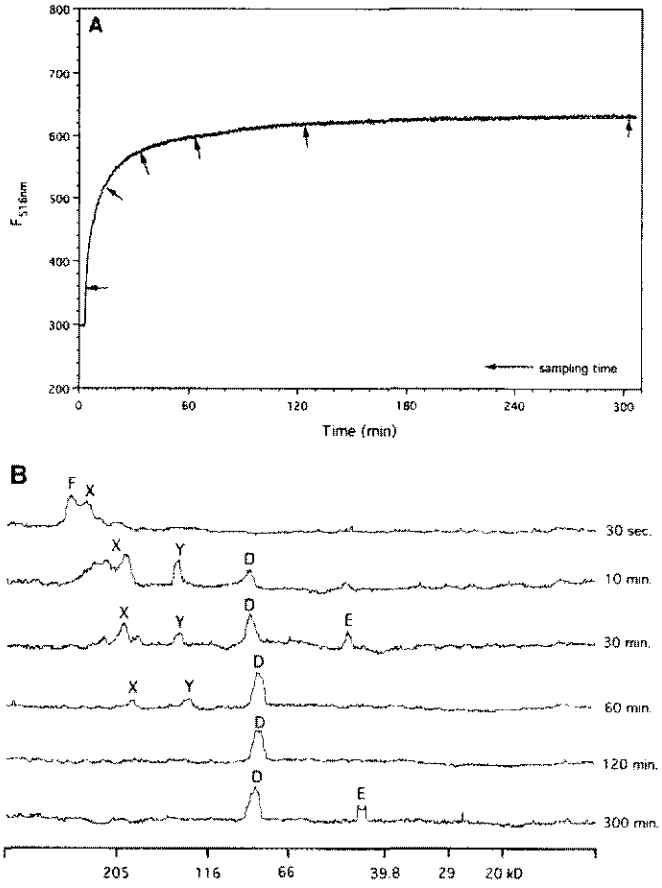

FIG. 3. Fluorescence intensity of 250 nM FITC–fibrinogen and 750 nM unlabeled fibrinogen upon addition of 10 nM plasmin (A). Small samples were removed at various times during fibrinogen degradation (as indicated by arrow) and subjected to SDS/PAGE, silver staining, and densitometry. Density scans are shown for various times of the reaction (B). During the reaction, fibrinogen (F) was degraded to fragment X, Y, D, and E as indicated.

Fibrinogenolysis

The action of plasmin on FITC–fibrinogen produced a large increase in fluorescence intensity in a plasmin-dependent manner. The degradation events which resulted in dequenching were studied via SDS/PAGE. Fluorescence scanning of a late digest separated by SDS/PAGE indicated that each major fragment was fluorescent. The major extent and most rapid rate of dequenching occurred at the earliest reaction times which correlated temporally with the degradation of fibrinogen to fragment X species during the first three minutes of the reaction (Figs. 3A and 3B). Fragment Y first became visible by silver-stained SDS/PAGE after 3 min when over 50% of the dequenching had already occurred. Fragment Y reached its maximal concentration between 10 and 30 min after digestion was initiated when the dequenching rate had already slowed considerably. The obtainment of the final extent of dequenching was seen at 60 min and occurred concomitantly with the presence of the last remaining fragment X in the digestion.

During fibrinogenolysis, the total fluorescence emission at any time is related to the amount of fluorescent fibrinogen and the amount of individual fluorescent degradation products in the sample. The intensity of fluorescence emission $F(t)$ is described by

$$F(t) = \alpha[\text{fbg}(t)] + \sum \beta_i \cdot [\text{FDP}_i(t)], \qquad [1]$$

where

$$i = X, Y, D, E, \text{ etc. and}$$

$$\alpha = F(0)/[\text{fbg}(0)] \text{ at } t = 0.$$

The majority of the dequenching occurs temporally during the generation of fragment X. Thus, an initial reaction rate analysis would relate the rate of dequenching with the first reaction step—the rate of fragment X generation. We conclude that all degradation fragments have approximately the same fluorescence intensity per molecule, β, which is justified by the fact that the de-

quenching signal reaches steady state long before lysis is complete—conversion of the Y fragment to D fragment produced little additional dequenching. Plasmin degradation of one fibrinogen molecule can produce *at least* three dequenched fragments that include a single X fragment and *at least* two small fragments from the carboxy terminus of the α chains. For the reaction where plasmin converts one quenched fibrinogen molecule to n dequenched fragments (of different size, but same β) with $n \geq 3$, Eq. [1] becomes

$$F(t) = \alpha[\text{fbg}(t)] + \beta \cdot [n \text{ dequenched fragment } (t)] \quad [2a]$$

or

$$F(t) = \alpha[\text{fbg}(t)] + \beta' \cdot [\text{X}(t)] \quad [2b]$$

where

$$\beta' = \beta\, n \text{ and}$$

$$\beta' = F_{\max}/[\text{fbg}(0)] \text{ as all fibrinogen} \rightarrow \text{X}.$$

Differentiating Eq. [2b] where $[\text{fbg}(0)] = [\text{fbg}(t)] + [\text{X}(t)]$, the rate of dequenching is related to X generation by Eq. [3]. One measure of the consistency of this approach is that the expression $[\text{fbg}(0)]/(F(0) - F_{\max})$ which is equal to $1/(\alpha - \beta')$ remained constant as expected, regardless of reaction conditions.

$$\frac{1}{(\alpha - \beta')}\frac{dF}{dt} = \frac{d[\text{fbg}]}{dt} = -\frac{d[\text{X}]}{dt}. \quad [3]$$

For kinetic analysis where reversible binding and dissociation occurred by distinct binding sites separate from the catalytic site, the rate of complex formation is described by (19)

$$d[\text{plm}^b]/dt = k_f[\text{plm}^f]\,[\theta_{\text{plm}} - \text{plm}^b] - k_r[\text{plm}^b], \quad [4]$$

where the total available plasmin binding site concentration, θ_{plm} is equal to $q \cdot [\text{fbg}]$ and $q = 2$ initially for two plasmin binding sites per fibrinogen molecule (25). At all times, the free plasmin concentration $[\text{plm}^f]$ plus the bound plasmin concentration $[\text{plm}^b]$ is equal to the initial plasmin concentration $[\text{plm}^0]$. For rapid binding that equilibrates quickly ($d[\text{plm}^b]/dt = 0$), the concentration of bound plasmin is given by:

$$[\text{plm}^b] = (K_d + [\text{plm}^0] + q[\text{fbg}^0])/2 - \frac{\sqrt{(K_d + [\text{plm}^0] + q[\text{fbg}^0])^2 - 4\,q[\text{fbg}^0][\text{plm}^0]}}{2} \quad [5]$$

and the initial reaction rate is given as:

$$v = k_{\text{cat}} \cdot [\text{plm}^b]. \quad [6]$$

Using this model, as the initial concentration of fibrinogen increases to very large values (at constant plasmin concentration), the maximum reaction rate goes to $v_{\max} = k_{\text{cat}} \cdot [\text{plm}^0]$. As the initial plasmin concentration increases (at constant fibrinogen concentration), the maximum reaction rate goes to $v_{\max} = k_{\text{cat}} \cdot q[\text{fbg}^0]$.

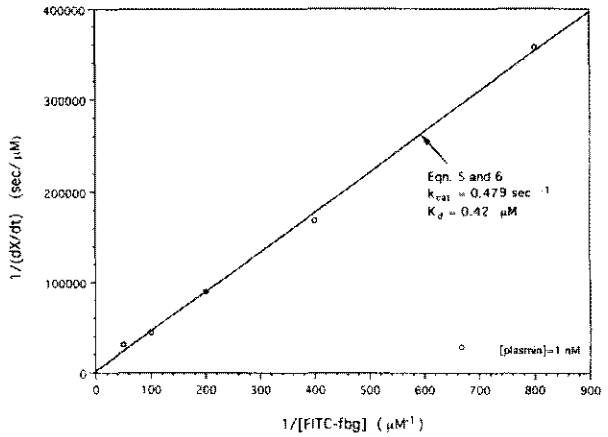

FIG. 4. Reciprocal plot showing the effect of fibrinogen concentration on plasmin-mediated fibrinogenolysis. Various concentrations of FITC-fibrinogen from 1.25 to 20 nM were digested with 1.0 nM plasmin. The initial rate of dequenching (dF/dt) was related to the rate of fragment X generation (dX/dt, μM/s) using Eq. [3] in the text. In all instances, initial rates were highly linear ($r^2 > 0.998$) for over 70 s after addition of plasmin. The theoretical curve using Eqs. [5] and [6] is shown for $k_{\text{cat}} = 0.479\ \text{s}^{-1}$ and $K_d = 0.42\ \mu\text{M}$.

Using 1 nM plasmin and varying concentrations of fibrinogen from 1.25 to 20 nM, we conducted a kinetic analysis for the generation of fragment X. A reciprocal plot is given for the initial rate of fragment X generation (Fig. 4) calculated from Eq. 3. A linear regression of the experimental data allowed direct calculation of the $v_{\max}$ and a determination of $k_{\text{cat}} = 0.479\ \text{s}^{-1}$. Using Eqs. [5] and [6], the K_d of active plasmin binding to fibrinogen was then calculated to be 0.42 μM.

Although enzyme assays are typically conducted under conditions of excess substrate, the sensitivity of fluorescence-based systems allowed the study of excess plasmin on nanomolar concentrations of fibrinogen. The fibrinogen substrate has two binding sites for plasmin, each with fairly high affinity for plasmin. Thus, it is expected that under the conditions of excess plasmin, these binding sites can be saturated with plasmin. This was indeed observed experimentally for the initial stage of the reaction when the ratio of plasmin to fibrinogen exceeded twice that of the initial concentration of fibrinogen (Fig. 5). Using values of $k_{\text{cat}} = 0.479\ \text{s}^{-1}$ and $K_d = 0.42\ \mu\text{M}$ obtained previously, we accurately predicted with Eqs. [5] and [6] the kinetic rates for reactions where the plasmin/fibrinogen ratio was less than one. A large deviation from the model was observed when the plasmin was in excess of the initial fibrinogen. Given the number of lysine binding sites per fibrinogen molecule, the measured reaction rates reached saturation at the expected plasmin concentrations, but the value of that maximum rate was considerably less than predicted. This may be due to the very short linear regime of the initial rate and the rapid destruction of fibrinogen such that the assumption of local binding equilibrium does

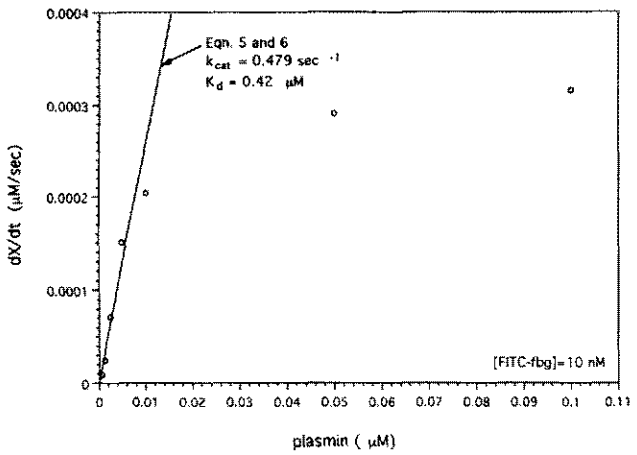

FIG. 5. Effect of increasing plasmin concentration on the initial rate of fragment X generation at constant concentration of fibrinogen (10.0 nM). The initial rate of dequenching (dF/dt) was related to the rate of fragment X generation using Eq. [3] in the text. In all instances, initial rates were highly linear ($r^2 > 0.997$) for over 10 s after addition of plasmin. The theoretical curve using Eqs. [5] and [6] is shown for $k_{cat} = 0.479\ s^{-1}$ and $K_d = 0.42\ \mu M$.

not hold or the initial concentration of fibrinogen cannot be used in Eq. [5] since it drops so rapidly at high plasmin concentration.

We found that preincubation of plasmin with ϵACA (10 mM) prior to addition to fibrinogen greatly reduced the dequenching rate which suggests that plasmin must bind fibrinogen in order to initiate lysis (Fig. 6A). This preparation of ϵACA–plasmin remained active on chromogenic substrates (chromozym PL). Addition of excess ϵACA after plasmin-mediated fibrinogenolysis was initiated resulted in a dose-dependent inhibition of dequenching (Fig. 6B). Addition of ϵACA (10 mM) immediately inhibited the progression of fibrinogenolysis as indicated by the cessation of dequenching. This indicated that plasmin can be removed from fibrinogen either by ϵACA disruption of the fibrinogen–plasmin complex or by ϵACA capture of desorbing plasmin. Addition of 10 nM plasmin to a mixture of 10 mM ϵACA and 20 nM FITC–fibrinogen resulted in a competition between free plasmin binding with fibrinogen and plasmin binding with ϵACA. In that competition, some plasmin was able to bind fibrinogen as indicated by the initial rate of dequenching (data not shown).

Fibrinolysis

During fibrinolysis, the dequenching of dissolving fibrin is more difficult to describe since the initial state of the substrate is quenched by three mechanisms: interactions within the monomer, monomer–monomer interactions in the protofibril, and fibril–fibril interactions in the fiber. During fibrinolysis, the monomers in the fibrils are degraded with subsequent loss of fibril/fiber structure. The early dequenching during fibrinolysis is due to the loss of quenching in the fibril/fiber and the generation of dequenched degradation products. The initial rate of dequenching was very similar for lysis of coarse and fine fibers (Fig. 7) and was dependent on the concentration of fibrinogen used at constant plasmin concentration. As seen in Fig. 1, the final dequenched state of lyzed fibrin (noncrosslinked) achieved a final fluorescence emission identical to the final dequenched state of lyzed fibrinogen. A kinetic analysis as conducted for fibrinolysis was not possible since various factors influence the rate of dequenching; however, the initial rate of fluorescence change for FITC–fibrin appeared similar to that seen for FITC–fibrinogen.

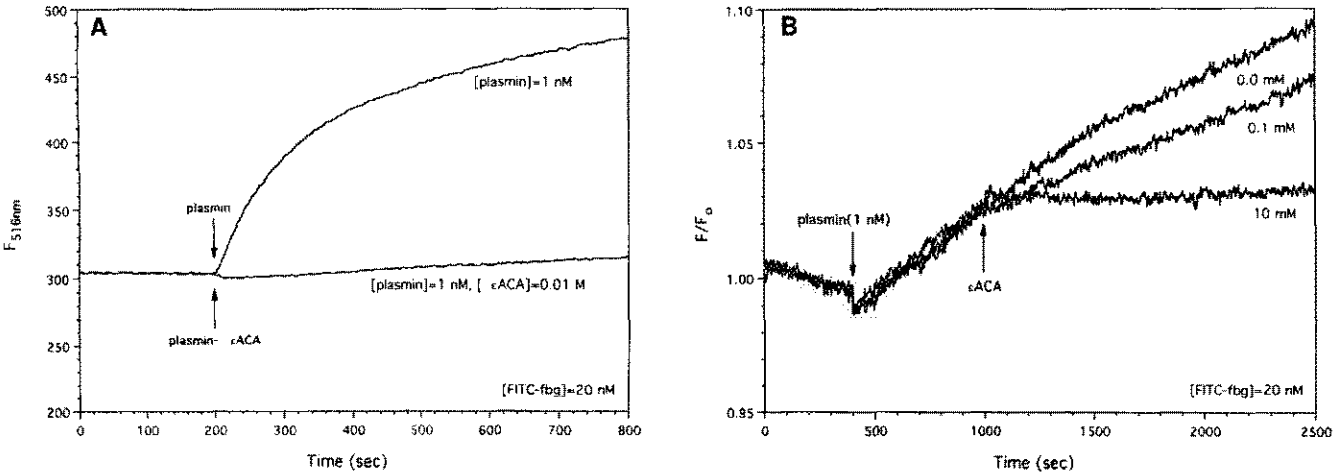

FIG. 6. Addition of ϵACA–plasmin complex to FITC–fibrinogen caused essentially no dequenching in comparison an equal amount of plasmin (1.0 nM) added to FITC–fibrinogen (A). Addition of 0.1 to 10 mM ϵACA to fibrinogen (20 nM) undergoing degradation by plasmin (1.0 nM) resulted in a dose-dependent inhibition of dequenching (B).

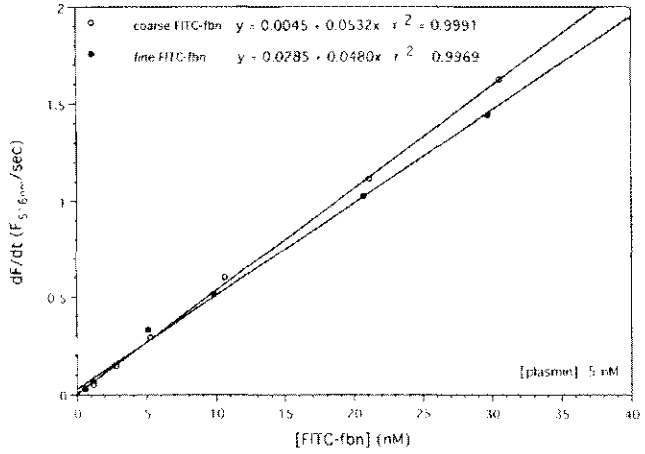

FIG. 7. Effect of fibrin concentration on the initial rate of dequenching by 5.0 nM plasmin. FITC–fibrinogen (80 nM) was polymerized using 1.0 U/ml thrombin at 0.1 M NaCl (coarse) or 0.3 M NaCl (fine) to create fibrin fibers. Aliquots of the polymerization mixture (0.5 to 30 nM equivalent FITC–fibrin monomer) were resuspended in a reaction buffer prior to addition of plasmin. In all instances, initial rates were highly linear ($r^2 > 0.996$) for over 40 s after addition of plasmin.

DISCUSSION

Extensive data are available for the kinetics of chromogenic substrate cleavage by glu- and lys-plasmin. However, these types of experiments do not allow the exploration of binding interactions and macromolecular structure that are critical to the regulation and rate of fibrinolysis. Lysis experiments are difficult to follow in real-time and typically require the use of isotopes and electrophoretic separations. The use of a fluorescence quenching and dequenching assay allows the real-time monitoring of very dilute systems (nM) under well-mixed conditions. The results of the polymerization and lysis assays that we conducted were qualitatively and quantitatively similar to optical density measurements conducted at micromolar concentrations of fibrin(ogen).

In considering the molecular proximity of monomers in the fibril and the nature of quenching of fine and coarse fibers, we suggest that the quenching during polymerization is due to fibril extension with fiber aggregation playing an additional important role. The deconvolution of the signal was not possible. Nonetheless, the quenching is the result of molecular proximity of labeled monomers at a "crowdedness" not achieved in solution prior to polymerization. Although the fiber aggregate is 80% water and the fibrils in the fiber are on average separated by significant distances (~5 to 25 nm), the fibrils may transiently interact closely, resulting on average with an aggregate-based quenching.

Based on electron microscopy analysis of fibrin, Veklich *et al.* (26) recently demonstrated that the carboxy-terminus domain of the α chains (αC) of fibrinogen are in close proximity to each other and to the E domain. These workers report that the αC domains move away from each other and from the E domain upon generation of the fibrin monomer (FPA and FPB release), but that αC domains of monomers closely interact during polymerization. These structural changes observed by electron microscopy are consistent with our observation that (i) fragment X generation from fibrinogen or fibrin results in strong fluorescence dequenching and (ii) polymerization leads to fluorescence quenching. The conformational changes of the αC domain away from the E domain during fibrinopeptide release (26) would be expected to produce dequenching in our assay system. Dequenching during thrombin polymerization was not observed, perhaps due to masking by the large quenching that accompanies polymerization. We have found that polymerization of FITC–fibrinogen by 1 U/ml of thrombin in the presence of 0.1, 10, and 100 μM Gly-Pro-Arg-Pro—a peptide that prevents polymerization (27)—reduced in a dose-dependent manner the rate and extent of quenching associated with polymerization. Over 80% of the thrombin-induced quenching was prevented when 100 μM GPRP was added before polymerization. Under conditions of inhibited polymerization using 100 μM GPRP, we observed only a very small amount of dequenching (~1% increase in fluorescence) upon fibrinopeptide release by 1 U/ml thrombin. The nonspecific nature of the FITC labeling used in the assay may have precluded the adequate probing of more subtle intramolecular conformational changes that have been observed by electron microscopy (26).

There are little kinetic data available for the actual rate constants of fibrinolysis. Such determinations would require information regarding dynamic bound plasmin concentrations, dynamic binding site concentrations, and release rates of plasmin from degraded fibrin. We have used a kinetic analysis based on the assumption of local binding equilibrium to estimate the rate of fragment X generation during plasmin-mediated fibrinogenolysis as $dX/dt = 0.479\ s^{-1} \cdot$ [bound plasmin]. This rate of fragment X generation is considerably slower than that seen for the cleavage of chromogenic substrates. However, the avidity of active plasmin binding to fibrinogen is fairly strong compared to that of chromogenic substrates. We calculated the K_d of active plasmin binding to fibrinogen to be 0.42 μM which is consistent with the measured value of active-site inhibited glu- or lys-plasmin binding to fibrin (K_d = 0.5 to 10 μM) (28) or the binding of lys-plasminogen to fibrin (K_d = 0.32 μM) (25). However, Lucas *et al.* (25) found that lys-plasminogen had a very weak interaction with fibrinogen (K_d = 1 mM). Our study with ϵACA suggests that during early lysis when the fibrinogen is largely intact (little Y, D, or E generated), the action of bound plasmin can be blocked with excess ϵACA in a dose-dependent and rapid manner (Fig. 6B). This suggests that plasmin can be desorbed from degraded fibrinogen either by

ϵACA disruption of the fibrinogen–plasmin complex or by ϵACA capture of transiently desorbing plasmin.

The dequenching method for following fibrinolysis and fibrinogenolysis reported the earliest kinetic event prior to complete degradation. In no experiments was a lagtime detected after plasmin was added to the samples. In future work, it may be possible to isolate and fluorescently label fragment X or Y such that these fragments would be suited for the kinetic study of X to Y and Y to D + E conversion. Coupled with measurements of adsorption/desorption rate constants, fluorescence dequenching may be useful for the evaluation of intrinsic rates based on the bound concentrations of enzyme.

In summary, the quench and dequench assay method exploits the sensitivity of fluorescence detection allowing the measurement of kinetic phenomena using reagent concentrations at the nanomolar level on substrates of physiological relevance. A single substrate (FITC–fibrinogen) can be used for study of fibrinogen polymerization, fibrinogenolysis, or fibrinolysis. Additionally that assay is easily adapted for studies of plasminogen activation on FITC–fibrin. When the binding and macromolecular complex formation are important, the use of fluorescence quenching and dequenching assay provides for possibilities not obtainable with chromogenic or fluorogenic substrates.

ACKNOWLEDGMENTS

The authors thank Dr. Frank Bright for helpful discussions. This work was supported by a National American Heart Association Grant 938670. Dr. Diamond is a recipient of the National Science Foundation National Young Investigator Award.

REFERENCES

1. Lottenberg, R., Christensen, U., Jackson, C. M., and Coleman, P. L. (1981) *Methods Enzymol.* **80,** 341–361.
2. Harpel, P. C., Chang, T. S., and Verderber, E. (1985) *J. Biol. Chem.* **260,** 4432–4440.
3. Fears, R. (1989) *Biochem. J.* **261,** 313–324.
4. deVries, C., Veerman, H., and Pannekoek, H. (1989) *J. Biol. Chem.* **264,** 12604–12610.
5. Takagi, T., and Doolittle, R. F. (1975) *Biochemistry* **14**(5), 940–946.
6. Pizzo, S. V., Schwartz, M. L., Hill, R. L., and McKee, P. A. (1972) *J. Biol. Chem.* **247,** 636–645.
7. Pizzo, S. V., Schwartz, M. L., Hill, R. L., and McKee, P. A. (1973) *J. Biol. Chem.* **248,** 4574–4583.
8. Mihalyi, E. (1983) *Ann. NY Acad. Sci.* **77,** 61–69 (1983)
9. Ranby, M., and Brandstrom, A. (1988) *in* Tissue-type Plasminogen Activator (t-PA) (Kluft, C., Ed.), pp. 211–224, CRC Press, Boca Raton, FL.
10. Gabriel, D. A., Muga, K., and Boothroyd, E. M. (1992) *J. Biol. Chem.* **267,** 24259–24263.
11. Weisel, J. W., and Nagaswami, C. (1992) *Biophys. J.* **63,** 111–128.
12. Blomback, B., Carlsson, K., Hessel, B., Liljeborg, A., Procyk, R., and Aslund, N. (1989) *Biochim. Biophys. Acta* **997,** 96–110.
13. Carr, M. E., Shen, L. L., and Hermans, J. (1977) *Biopolymers* **16,** 1–15.
14. Carr, M. E., and Hermans, J. (1978) *Macromolecules* **11,** 46–50.
15. Carr, M. E., and Hardin, C. L. (1987) *Am. J. Physiol.* **253,** H1069–1073.
16. Shah, G. A., Nair, C. H., and Dhall, D. P. (1985) *Thromb. Res.* **40,** 181–188.
17. Voter, W. A., Lucaveche, C., and Erickson, H. P. (1986) *Biopolymers* **25,** 2375–2384.
18. Blinc, A., Planinsic, G., Keber, D., Jarh, O., Lahajnar, G., Zidansek, A., and Demsar, F. (1991) *Thromb. Haemostasis* **65,** 549–552.
19. Diamond, S. L., and Anand, S. (1993) *Biophys. J.* **65,** 2622–2643.
20. Wu, J. H., and Diamond, S.L (1994)*Thromb. Haemostasis* **72,** 105–112.
21. Kanai, S., Okamoto, H., Tamaura, Y., Yamazaki, S., and Inada, Y. (1979) *Thromb. Haemostasis* **42,** 1153–1158.
22. Husain, S. S., Hasan, A. A. K., and Budzynski, A. Z. (1989) *Blood* **74,** 999–1006.
23. Genton, E., Fletcher, A. P., Alkjaersig, N., and Sherry, S. (1964) *J. Lab. Clin. Med.* **64,** 313–320.
24. Maeda, H., Ishida, N., Kawauchi, H., and Tuzimura, K. (1969) *J. Biochem.* **65,** 777–783.
25. Lucas, M. A., Fretto, L. J., and McKee, P. A. (1983) *J. Biol. Chem.* **258,** 4249–4256.
26. Veklich, Y. I., Gorkun, O. V., Medved, L. V., Nieuwenhuizen, W., and Weisel, J. W. (1993) *J. Biol. Chem.* **268,** 13577–13585.
27. Laudano, A. P., and Doolittle, R. F. (1978) *Proc. Natl. Acad. Sci. USA* **75,** 3085–3089.
28. Suenson, E., and Thorsen, S. (1981) *Biochem. J.* **197,** 619–628.